

Vilniaus universitetas  
Fizikos fakultetas  
Taikomosios elektrodinamikos ir telekomunikacijų institutas

Gustas Levickis  
OKSIDINIŲ KERAMIKŲ ELEKTRINIŲ SAVYBIŲ TYRIMAI

Bakalauro studijų baigiamasis darbas

Šviesos technologijų studijų programa

Studentas

Gustas Levickis

Leista ginti

2024-01-10

Darbo vadovas

dr. Vilma Kavaliukė

Instituto direktorius

dr. Robertas Grigalaitis

Vilnius 2024

Vilnius University  
Faculty of Physics  
Institute of Applied Electrodynamics and Telecommunications

Gustas Levickis  
ELECTRICAL PROPERTIES INVESTIGATION OF SOME OXIDE CERAMICS

Bachelor's final thesis

Light Engineering study programme

Student

Gustas Levickis

Approved

2024-01-10

Academic supervisor

dr. Vilma Kavaliukė

Director of the Institute

dr. Robertas Grigalaitis

Vilnius 2024

# Table of Contents

1. Introduction .....	4
2. Literature Review .....	5
2.1 Solid Oxide Fuel Cells .....	5
2.2 Oxygen ion conductive solid electrolytes and doping .....	6
2.3 Ceria Based Ceramics Solid Electrolytes .....	7
3. Experimental.....	9
3.1 Preparation of ceramics.....	9
3.2 Sample preparation .....	11
3.3 The basic principals of impedance spectroscopy.....	11
3.4 Equivalent circuits and modelling .....	13
4. Results and discussion.....	15
5. Conclusions .....	24
6. Bibliography .....	25
Summary.....	27
Santrauka .....	28

## 1. Introduction

Cerium oxide ceramics doped with various elements are being investigated with a view to their application in solid oxide fuel cells (SOFCs), in which the solid electrolyte is one of the main components and which must be both electron-impermeable and have a high ionic conductivity of oxygen vacancies [1–3].

Samaria or gadolinia or both samaria and gadolinia doped ceria (SDC, GDC, SGDC) ceramics belong to the group of oxygen vacancy solid electrolytes (characterized by a high oxygen ionic conductivity). Other than composition, one of the main factors influencing the electrical conductivity of the ceramics is their microstructure, such as crystallite size and composition of the grain boundary. Microstructure can be influenced by the choice of the conditions in which the ceramics are manufactured, such as the method of powder synthesis, the time and temperature of the sintering of the ceramic. [3]

Various dopant elements (Gd, Sm [4], Nd, Lu [5], Y, La [6]) are used in ceria to increase its ionic conductivity. The highest conductivities were reported to be achieved with Gd and Sm dopants. [4]

A high ionic conductivity was reported for samaria and gadolinia co-doped ceria (SGDC). It was reported to be higher than of individually doped ceria ceramics. [4]

The aim of this work was to investigate electrical conductivity of oxygen ion conductive ceramics and the influence of synthesis method and sintering conditions on the electrical conductivities of ceria-based ceramics.

This was achieved by the investigation of the electrical properties (activation energies for grain and total electrical conductivities and values of grain and total electrical conductivities) of some oxide ceramics, mainly in the doped ceria family.

Influence of powder synthesis method, sintering temperature was investigated. Evaluated the results to find highest electrical conductivity at lower temperatures (500K, which is typical for intermediate temperature SOFCs) due to issues arising for SOFCs operated at high temperatures [1,7].

## 2. Literature Review

### 2.1 Solid Oxide Fuel Cells

Solid oxide fuel cells (SOFCs) - electrochemical devices that convert chemical energy into electrical energy by utilizing a chemical fuel and oxygen as the oxidizing gas. Comprised of two porous electrodes (anode and cathode) and a solid electrolyte, the electrodes play a crucial role in enabling the transfer of gases between the electrode/electrolyte interface in both directions. The main part of most devices is a thin dense membrane of an oxygen ion conductor (electrolyte) that separates the two chambers. The device can either be subject to an applied voltage whereby it will act as an oxygen pump or in the opposite way to generate electrical power as a SOFC. As the electrical energy is produced not by combustion but by electrochemical reaction, it is not limited by Carnot efficiency. As such, it is able to reach higher conversion efficiencies. [1,3,8]

An example SOFC system shown in Figure 1:

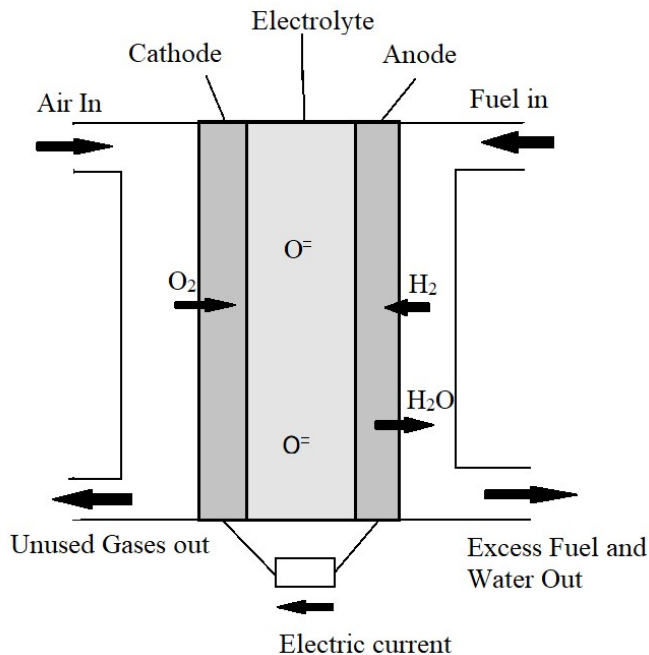


Figure 1. Scheme of a solid oxide fuel cell using hydrogen as fuel.

In the electrolyte of a SOFC (an oxygen ion conductor) the flow of current occurs due to movement of oxide ions through the lattice of the crystal. For a material to be a pure oxygen ion conductor (a solid electrolyte), any electronic contribution to total electrical conductivity must be insignificant as even the slightest concentrations of electronic carriers tend to give rise to a significant electronic

component. This is due to the comparatively high mobility of electrons and holes when compared to the ionic mobilities. [1]

The movement of oxygen ions in the crystal lattice is facilitated by thermally-activated hopping, allowing them to migrate from one crystal lattice site to another, with a drift of ions in the direction of the electric field. Thus, the ionic conductivity exhibits a strong dependence on temperature, with higher temperatures enabling high conductivity values. These levels of ionic conductivity at elevated temperatures are comparable to those observed in liquid electrolytes. [1]

High operating temperature is beneficial in enhancing the ionic conductivity of the electrolyte and, consequently, improving the electrochemical performance of the cell. However, high operating temperatures (800-1000°C) (such as those needed for yttrium stabilized zirconia ceramics) introduce a range of issues related to the materials, encompassing electrode sintering, catalyst poisoning, interfacial diffusion between electrolyte and electrode materials, thermal instability and the mechanical or thermal stresses arising from differing coefficients of thermal expansion among the cell components. [3,8]

## **2.2 Oxygen ion conductive solid electrolytes and doping**

To create solid electrolytes, doping is usually applied. It involves the substitution of lower-valence cations into the lattice, simultaneously introducing oxygen vacancies to ensure overall charge neutrality. These oxygen vacancies (equivalent sites) allow for the migration of oxygen ions and are crucial for achieving high ionic conductivity. [1,9]

Increasing the dopant concentration leads to the introduction of more vacancies into the lattice and one could assume that it should result in higher conductivity. While it would be a reasonable assumption that the maximum would be achieved at the point when half the oxygen lattice sites are vacant, the correlation of vacancies and conductivity only applies at low concentrations of dopant. A maximum is observed and conductivity drops when the vacancy concentration is only a few percent. [1,9]

The maximum is caused by the interaction of the oxygen vacancy and the substitutional ion. Utilizing modelling it was shown that the major interaction between these point defects is through the elastic strain in the crystal lattice introduced by a mismatch between the size of the dopant ion and the ion that it replaces. Thus, it appears that in order for good oxygen conductors to be made, the introduced vacancies should result in as little disturbance in the crystal lattice as is possible. This helps explain

why some of the best oxygen ion conductors are materials where the host and dopant ions barely differ in size. Examples include zirconia-scandia and ceria-gadolinia. [1]

Additional causes of this decrease in conductivity at higher concentrations of dopant ions include growth of defect clusters. And while the rise in dopant concentration leads to an increase in the quantity of charge carriers, it also results in defect interaction enhancement. This leads to a severe reduction in mobility. It shows that a lower dopant concentration results in the creation of oxygen vacancies, while a higher concentration results in a significant association between the oxygen and dopant vacancies. Optimal dopant concentration for ceria-based ceramics was suggested to be between 15 and 25 mol%. [9]

### **2.3 Ceria Based Ceramics Solid Electrolytes**

Fluorite oxides are oxygen ion conducting oxide materials, with the general formula of  $MX_2$ . The X ions occupy the eight tetrahedral interstitial sites whereas M ions occupy the regular sites of a face-centred cubic (FCC) structure. X being the large tetravalent cation. [1]

Materials that readily form in the fluorite crystal structure are such as thorium dioxide ( $ThO_2$ ), uranium dioxide ( $UO_2$ ) and in this work used ceria ( $CeO_2$ ). For zirconia, the  $Zr^{4+}$  cation is too small to sustain the fluorite structure and thus only forms at high temperatures or when there is partial substitution of the zirconium with another cation. The substituted cation is usually larger. [1]

A feature of the fluorite structure is its ability to sustain high degrees of substitution and the arising non-stoichiometry, allowing to obtain highly disordered materials. This structure has a relatively large interionic open space, allowing for high levels of point defects. [10]

Doping in fluorite oxides is usually achieved by substituting the host cation with either a rare earth or an alkaline earth metal. Examples include doped zirconias such as yttria-stabilized zirconia. Compositions when close to 10% of yttria is substituted show high electrical conductivities at temperatures of 800°C and above, making it a widely used electrolyte. It is of interest to find ceramics of high ionic conductivity at lower temperatures, such as gadolinia doped ceria (GDC). [1]

Thus, regarding doped ceria, highest conductivities have been reported for either gadolinia (GDC) or samaria doped ceria (SDC). It is reported that a conductivity of  $4.2 \text{ Scm}^{-1}$  was achieved in SDC ceramics at 700°C, while conductivity of GDC ceramics at 800°C was  $10 \text{ Scm}^{-1}$ . The ionic conductivity of SDC and GDC is higher than that of yttria-doped ceria. However, enhancement of stability in reducing conditions is still required for ceria-based electrolytes. [8,11]

Electrical conductivity in an oxide is influenced by several factors such as oxygen partial pressure in the surrounding gas atmosphere, temperature, concentration and type of dopants. Ion conduction in oxides is a thermally activated process, and between different materials its magnitude may vary significantly. That is why even the same matrix with different dopants can exhibit significant differences in the conductivity of ions. However, there is still a discrepancy in understanding how dopant properties precisely relate to ionic conductivity. [3]

For co-doped ceria, in this case samaria and gadolinia co-doped ceria (SGDC), a study found the bulk electrical conductivity to be even higher than that of singly doped ceria (GDC). Suggested cause for improvement was proposed to have a relation with the lowering of association enthalpy of the oxygen vacancy and the dopant ions. Other factors which were found to possibly have impact in the co-doping effect - modification of an elastic strain in the crystal lattice, raise of a configurational entropy and changes in the composition of the grain boundary. [11]

Another study claimed to have obtained better structural uniformity and structural homogeneity in ceria co-doped material (SGDC) when compared to singly gadolinia doped ceria and by usage of high-resolution transmission electron microscopy identified the presence of nanodomains in both materials, though less pronounced in the co-doped system. This study claimed nanodomains being a cause of high grain resistivity due to charge carriers being blocked in those areas. [3]

Co-doping in ceria (SGDC) is theorized to restrain the growth of large clusters and thus suppress local oxygen vacancy ordering, resulting in higher ionic conductivity due to the improvement of microstructural homogeneity. Additionally, it was presented stating that oxygen vacancies in the non-co-doped samples (SDC, GDC) being more tightly bound than in the samples with co-doping (SGDC), impeding effective oxygen ion conduction and having a direct effect on the conductivity. [3,12]

### 3. Experimental

#### 3.1 Preparation of ceramics

A number of ceria-based oxygen ion conductors were investigated. Different materials were obtained from different providers: Fuel Cell Materials, Kaunas University of Technology (KTU), University of Le Mans (obtained already sintered pellets). List of samples shown in Table 1. The material data sheets of the powders provided by Fuel Cell Materials did not mention powder synthesis method, although the powder grain size was characterized using BET (Brunauer–Emmett–Teller) analysis. Thus, as the synthesis method is not known, instead in Table 1 we provide BET.

Table 1. Sample notation, chemical composition, powder synthesis method/BET, sintering conditions (temperature T and time t), provider of powder.

Sample Name	Formula	Powder synthesis method/ BET	T (°C)	t (h)	Provider
GDC-1200-2h	$Ce_{0.9}Gd_{0.1}O_{1.95}$	BET=6.44 m <sup>2</sup> g <sup>-1</sup>	1200	2	Fuel Cell Materials
GDC-1500-2h	$Ce_{0.9}Gd_{0.1}O_{1.95}$	BET=6.44 m <sup>2</sup> g <sup>-1</sup>	1500	2	Fuel Cell Materials
GDC-1400-2h-ssr	$Ce_{0.9}Gd_{0.1}O_{1.95}$	Solid state reaction	1400	2	University of Le Mans
GDC-1400-2h-cp	$Ce_{0.9}Gd_{0.1}O_{1.95}$	Coprecipitation	1400	2	University of Le Mans
SDC-1500-2h	$Sm_{0.15}Ce_{0.85}O_{2-\delta}$	BET=8.04 m <sup>2</sup> g <sup>-1</sup>	1500	2	Fuel Cell Materials
SDC-1500-2h-n	$Sm_{0.15}Ce_{0.85}O_{2-\delta}$	BET=195 m <sup>2</sup> g <sup>-1</sup>	1500	2	Fuel Cell Materials
SGDC-1200-2h-cp	$Ce_{0.825}Sm_{0.0875}Gd_{0.0875}O_{2-\delta}$	Coprecipitation	1200	2	KTU
SGDC-1500-2h-cp	$Ce_{0.825}Sm_{0.0875}Gd_{0.0875}O_{2-\delta}$	Coprecipitation	1500	2	KTU

Commercial powders synthesized by Fuel Cells Materials or powders by KTU scientists (see Table 1) were pressed at 200 MPa into 8mm diameter pellets using press and press-form (Figure 2).

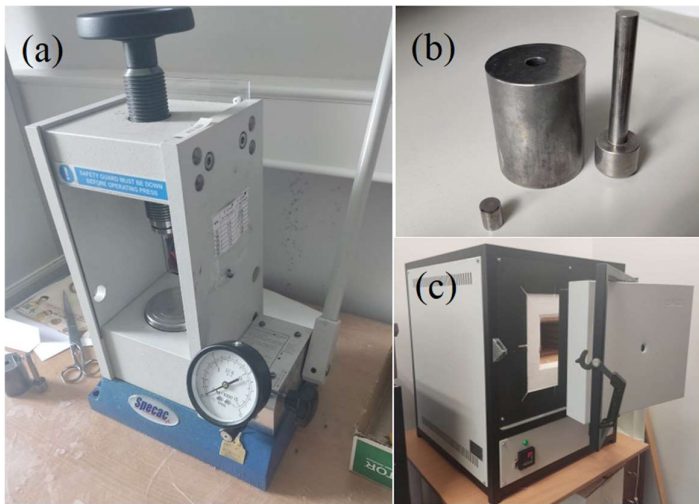


Figure 2. Equipment used in preparation of ceramics – press (a), press-form (b), furnace (c).

Each of these samples were first heated by  $2^{\circ}\text{C}/\text{min}$  to  $400^{\circ}\text{C}$  and held at this temperature for 1h to remove bound water, then heated by  $2^{\circ}\text{C}/\text{min}$  to  $1200^{\circ}\text{C}$  or  $1500^{\circ}\text{C}$  (depending on the sample) and sintered in ambient air at this temperature for 2h. For a typical sintering program see Figure 3. The samples were cooled down passively.

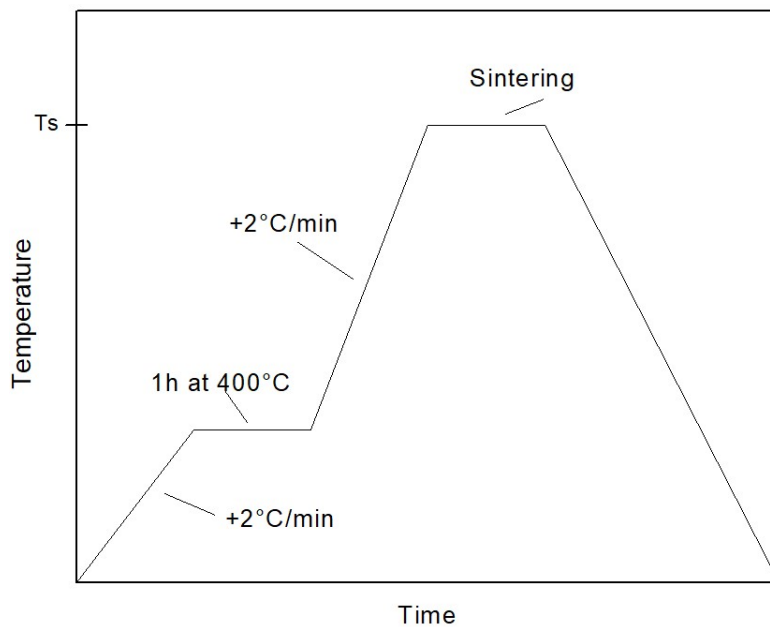


Figure 3. Sintering program for ceramic at sintered at sintering temperature ( $T_s$ ).

Samples from University of Le Mans were already obtained in sintered pellet form and thus no further sintering was needed. Sintering conditions can be seen in Table 1.

### 3.2 Sample preparation

For impedance spectroscopy measurements cylindrical samples of defined size are needed. The ceramic pellets were shaped down into workable shape (dimensions needed to fit into the spectrometer). Platinum contact paste (Mateck platinum conducting paste for brush application 71% Pt) was applied on the ends of the samples. The platinum contacts were first heated to and held at 400°C for 1h to evaporate contact paste solvent, followed by the contacts being fired on at 800°C for 20 min.

Example of sample with applied contacts shown in Figure 4.



Figure 4. SGDC-1500-2h-cp sample with platinum electrodes, 2.9mm diameter, 1.45mm height.

### 3.3 The basic principals of impedance spectroscopy

After the finished preparation, the ceramics were measured using an impedance spectrometer. It is known that for GDC and SDC ceramics oxygen transport for oxygen is very close to 1 [13].

Impedance can be seen as the complex resistance experienced by current flowing through a circuit composed of various electrical elements, such as inductors, capacitors and resistors, applying to both direct current (DC) and alternating current (AC). It, like resistance, is a ratio between voltage and current, showing the circuit's ability to resist electric current flow while also reflecting its ability to store electrical energy, referred to as “real impedance” and “imaginary impedance” accordingly. [14]

Measurement method used was ammeter-voltmeter two probe method. Impedance spectrometer used for most measurements is shown in Figure 5. It is capable of measurements in the 10 Hz to 2 MHz frequency range and 300 K to 800 K temperature range. It can perform measurements in frequency and time domains. [15]

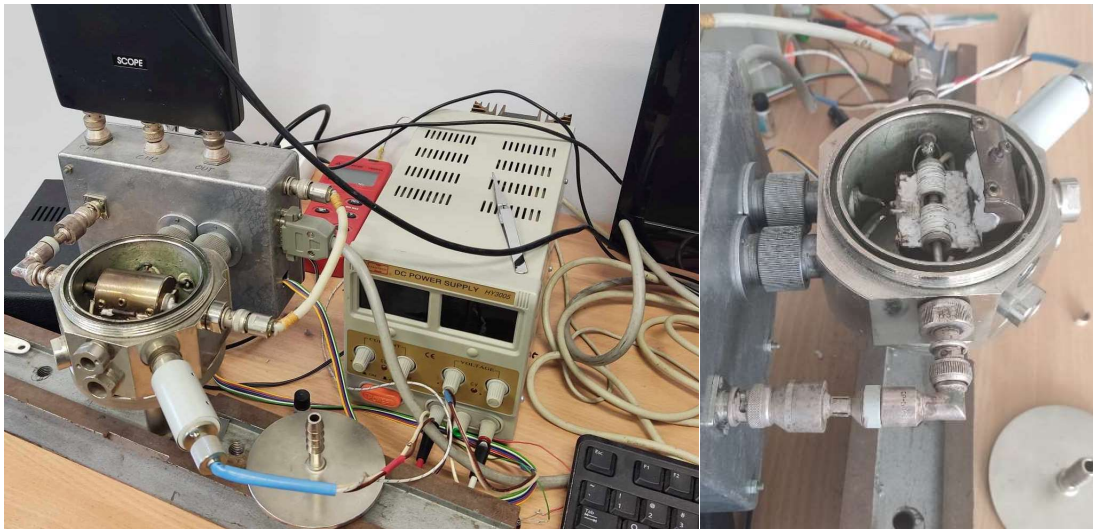


Figure 5. Impedance spectrometer setup and sample holder.

For samples GDC-1400-2h-ssr and GDC-1400-2h-cp a spectrometer capable of measurements at higher frequencies (0.3 to 10 GHz) was used, shown in Figure 6. [16]

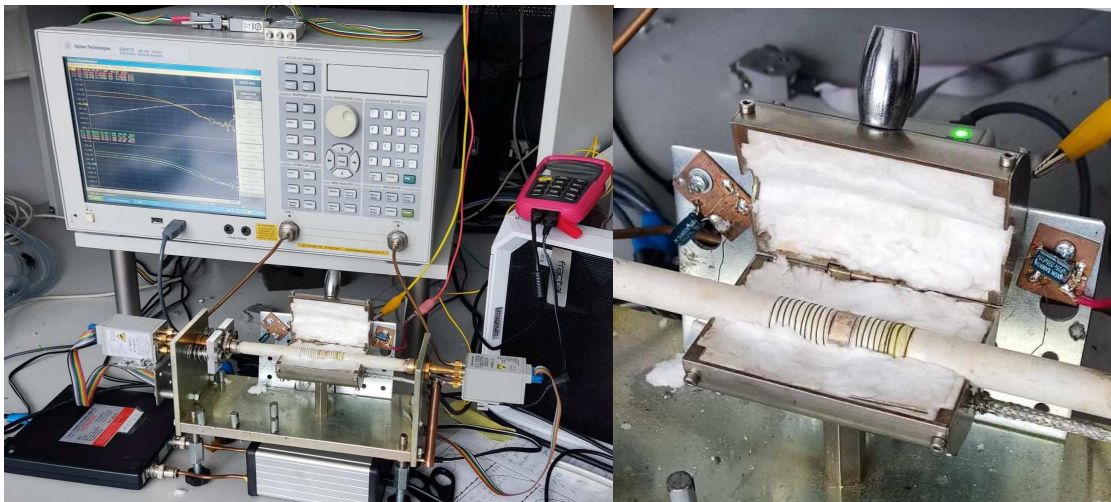


Figure 6. Higher frequency capable impedance spectrometer setup and sample holder.

### 3.4 Equivalent circuits and modelling

For the analysis of the obtained impedance spectroscopy results, the Bauerle brick layer model can be used. Here the solid electrolyte ceramic is imagined as a brick wall with the bricks being the crystallites and where the cement represents grain boundaries. The equivalent circuit (circuit which tries to model the complex electrical characteristics of a material by simple circuit elements) suggested by Bauerle in this model consists of three in series connected dual parallel connections of a resistor and capacitor, where the first of the parallel elements represent the grain ( $R_g$  and  $C_g$ ), the second ( $R_{gb}$  and  $C_{gb}$ ) the grain boundary and the third ( $R_{el}$  and  $C_{el}$ ) the electrode (Figure 7). [14]

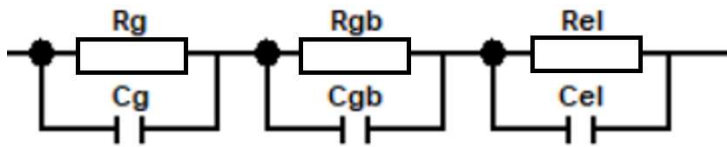


Figure 7. Equivalent circuit representing the Bauerle brick-layer model.

But these ideal equivalent circuit elements (resistors or capacitors) are not enough to adequately model the ceramic. Impedance spectra plotted as Nyquist plots often show depressed semicircles.

The introduction of "distributed" EC (equivalent circuit) elements enhances the representation of nonideal aspects in the modelled real-life processes. This accounts for observed deviations from ideal behaviour. When a potential is applied to a macroscopic system, the total current comprises of numerous microscopic current filaments that originate and terminate at the electrodes. In the presence of rough electrode surfaces or inhomogeneous dielectric materials, these microscopic current filaments may differ significantly (microscopic material properties themselves are often distributed). [17]

With electrode position, reaction resistance and capacitance contributions differing and varying over a certain range and around a mean, only the average effects over the entire surface of the electrode can be detected. For example, macroscopic impedance depends on the distribution of the reaction rate across such an interface which is measured as an average over the whole electrode. In response to a small-amplitude excitation signal, differences can lead to frequency-dependent effects, which can be often modelled using simple distributed circuit elements. [17]

The term "constant phase element" is derived from the fact that the phase angle of the circuit portion represented by such an element remains independent of AC frequency. [17]

Impedance of a CPE is dependent on effective CPE coefficient  $Q$  [ $\Omega^{-1}s^\alpha$ ], described in Equation 1:

$$Z_{CPE} = \frac{1}{Q(j\omega)^\alpha} \quad (1)$$

Equation 1 describes impedance response for ideal capacitor in case of  $\alpha=1$ , where  $\alpha$  – dimensionless parameter between 0 and 1, and an impedance response for an ideal resistor in case of  $\alpha=0$ .

Thus, we replace the capacitor in the Bricklayer model equivalent circuit (Figure 7) with a constant phase element (CPE). This is done as it represents an imperfect capacitor, as electrical circuit impedance analysis is an attempt to represent a complex phenomenon in purely electrical terms. While ideal circuit elements like resistors and capacitors can sometimes be employed by fitting the data, real systems often require the inclusion of distributed circuit elements (such as CPE) alongside the ideal ones to well characterize impedance responses [14].

## 4. Results and discussion

Obtained data was analysed using ZView Software, used for data analysis of impedance spectroscopy measurements and circuit modelling. The experimental values of grain resistivity and grain boundary resistivity at different temperatures have been obtained from the fits.

Sample grain and total resistivities were obtained by fitting to the data. Examples of data, equivalent circuits and fits show in Figures 8-9. In this software, the parameter  $\alpha$  from Equation 1 is noted as CPE-P, and the CPE coefficient Q denoted as CPE-T. In the shown equivalent circuits the elements noted CPE<sub>g</sub>, CPE<sub>gb</sub>, CPE<sub>el</sub> represent grain, grain boundary and electrode equivalent CPE elements respectively.

In Figure 8 we can see three semicircles. The one in the highest frequency represents ion relaxation in the grain, the middle one – in the grain boundary and the last one – in the electrode.

It can be clearly seen in Figure 9 that the ion relaxations of the electrode and the grain boundary overlap and thus separating them becomes difficult. The influence of the electrode is too strong in Figure 9 to obtain  $R_{gb}$  (at reasonable accuracy throughout the various temperatures) and thus obtain total resistivity.

From resistivity we can find conductivity. Grain conductivity ( $\sigma_g$ ) and total conductivity ( $\sigma_{tot}$ ) values were calculated with Equations 2-3:

$$\sigma_g = \frac{1}{R_g} \quad (2)$$

$$\sigma_{tot} = \frac{1}{R_g + R_{gb}} \quad (3)$$

where  $R_g$  – grain resistivity,  $R_{gb}$  – grain boundary resistivity.

As the relation of electrical conductivity and temperature changes according to the Arrhenius equation (Equation 4), it can be used to calculate the activation energies [14]:

$$\sigma = \sigma_0 \exp \frac{-\Delta E_\sigma}{kT}, \quad (4)$$

where  $T$  – absolute temperature,  $\sigma$  – conductivity,  $\sigma_0$  – pre-exponential factor,  $k$  – Boltzmann constant,  $\Delta E_\sigma$  - activation energy.

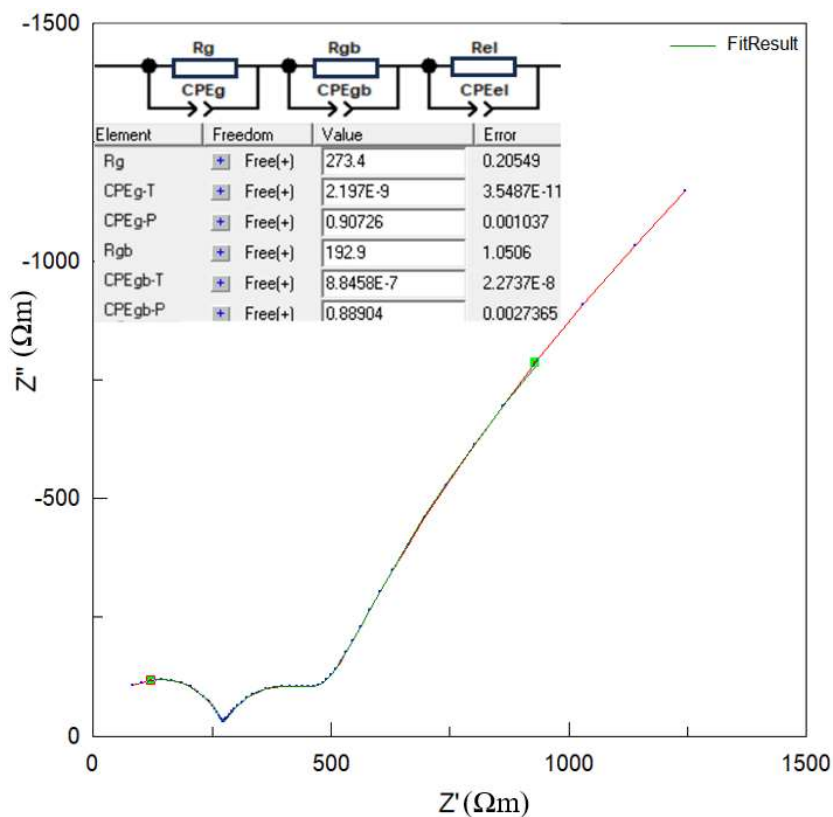


Figure 8. Nyquist plot of GDC-1500-2h ceramic at 500 K with fitted circuit and fit (green line).

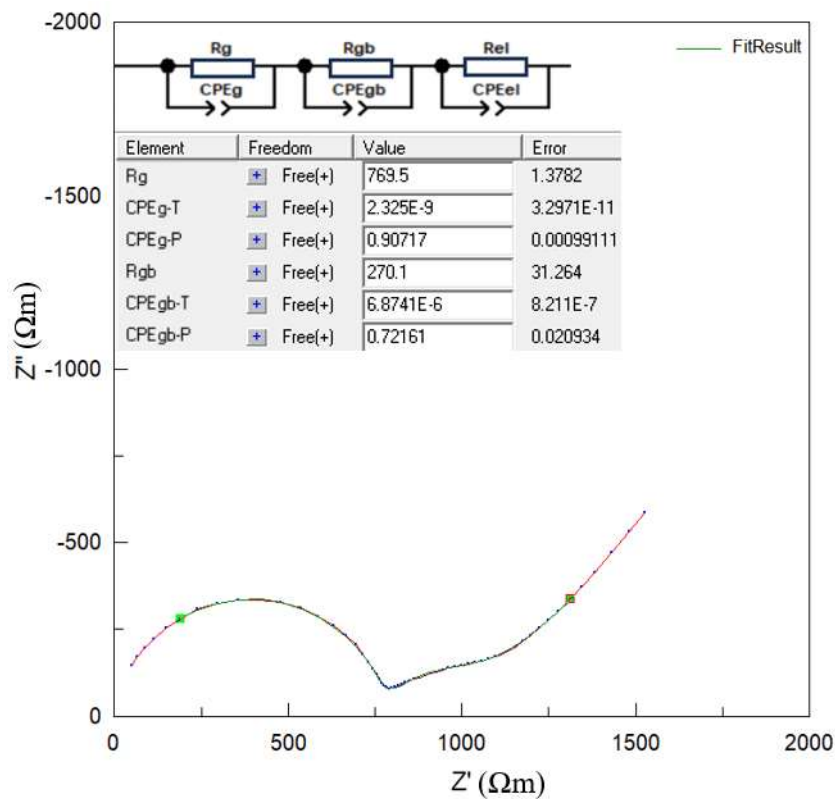


Figure 9. Nyquist plot of SGDC-1500-2h-cp ceramic at 500 K with fitted circuit and fit (green line).

In Figure 10 the imaginary part of the impedance for GDC-1500-2h at various temperatures can be seen. The maximum (at highest frequencies) is related to ion relaxation in crystallites and it shifts to even higher frequencies when the temperature is increased, almost fully disappearing from the measured frequency range at temperatures above 600 K.

The grain boundary ion relaxation is more difficult to separate, due to influence of the electrode. It also shifts to even higher frequencies when the temperature is increased, similarly being a thermally activated process.

Thus, it is clear we can not obtain the grain and grain boundary resistivities in the whole temperature range.

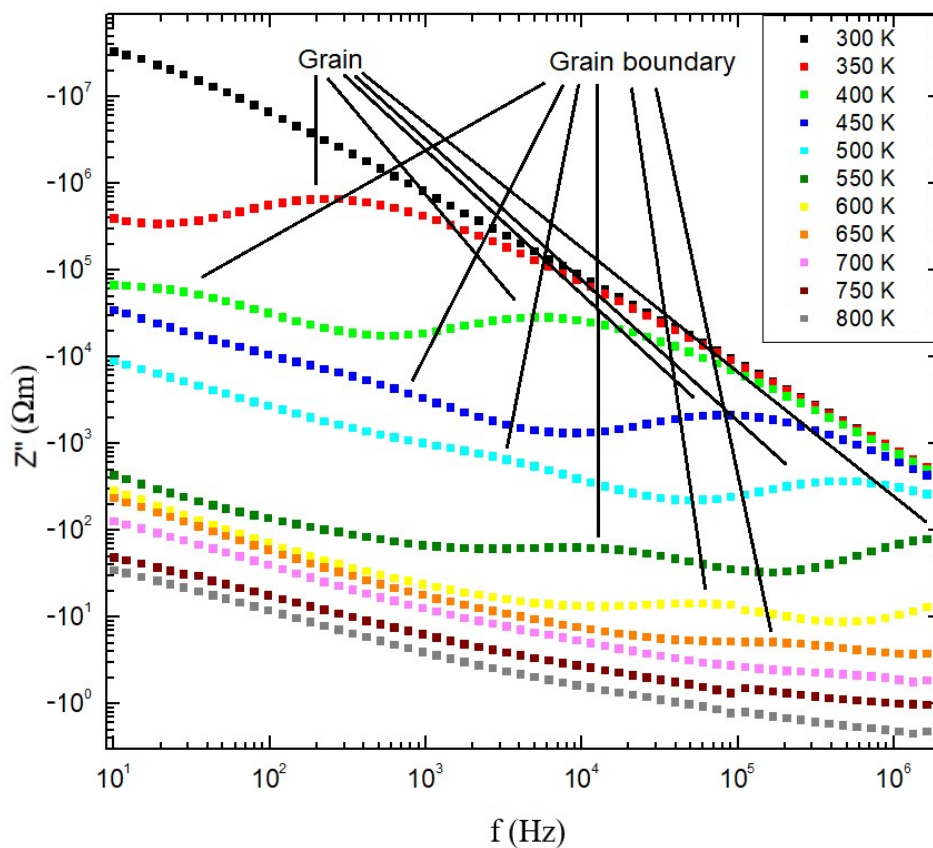


Figure 10. Dependence of the imaginary part of impedance on frequency for GDC-1500-2h ceramic for various temperatures. Grain and grain boundary maximums due to ion relaxation shown.

Figure 11 illustrates and compares all the measured GDC samples, their electrical conductivity with relation to reciprocal temperature. Figures 12-13 show the Nyquist plots for those ceramics.

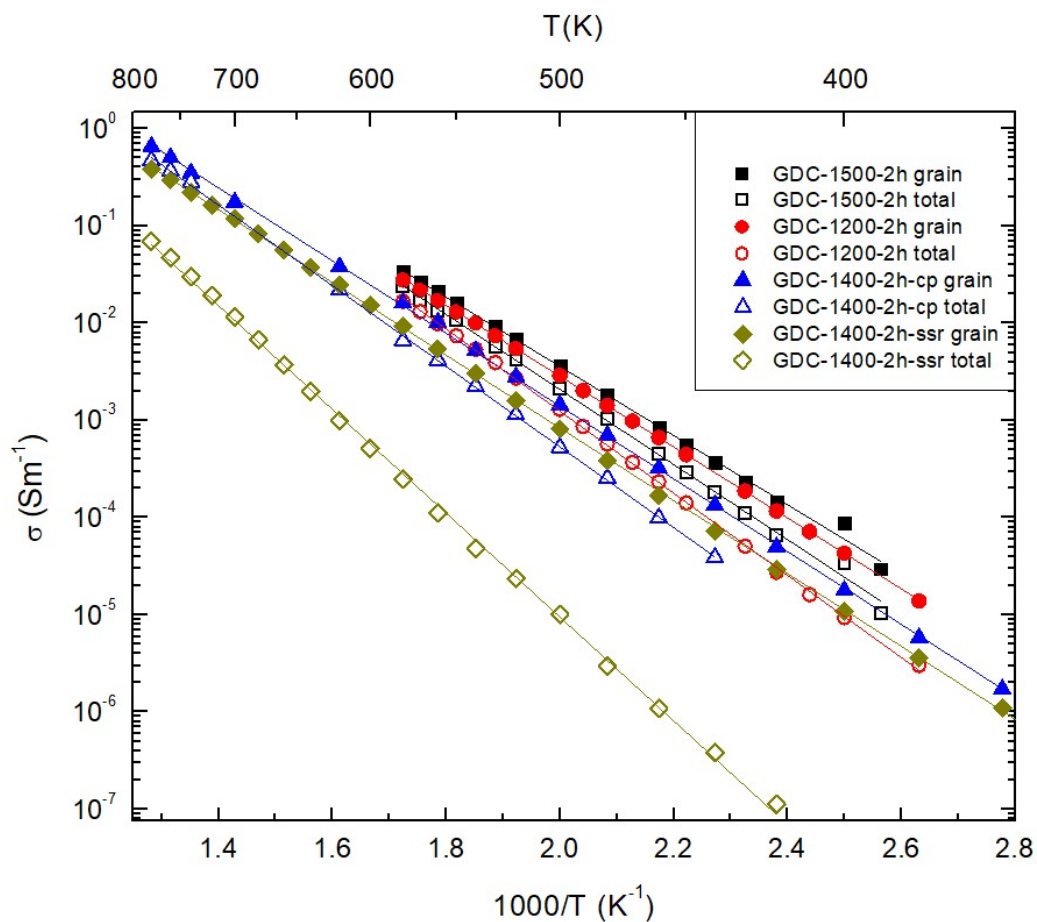


Figure 11. GDC ceramics grain and total electrical conductivity with relation to reciprocal temperature.

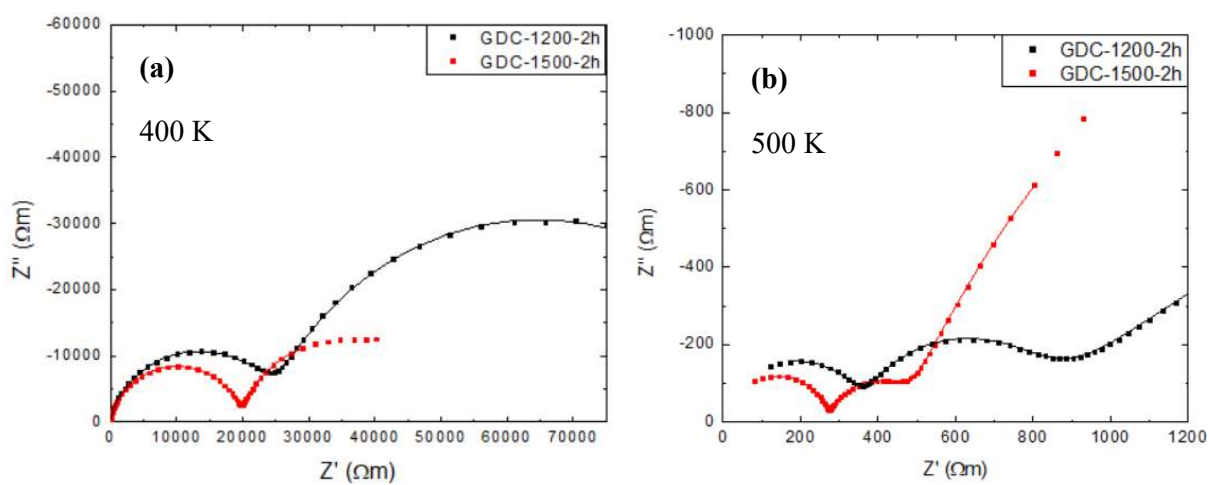


Figure 12. Nyquist plots with ZView fits of GDC-1200-2h and GDC-1500-2h at temperatures of 400 K (a) and 500 K (b).

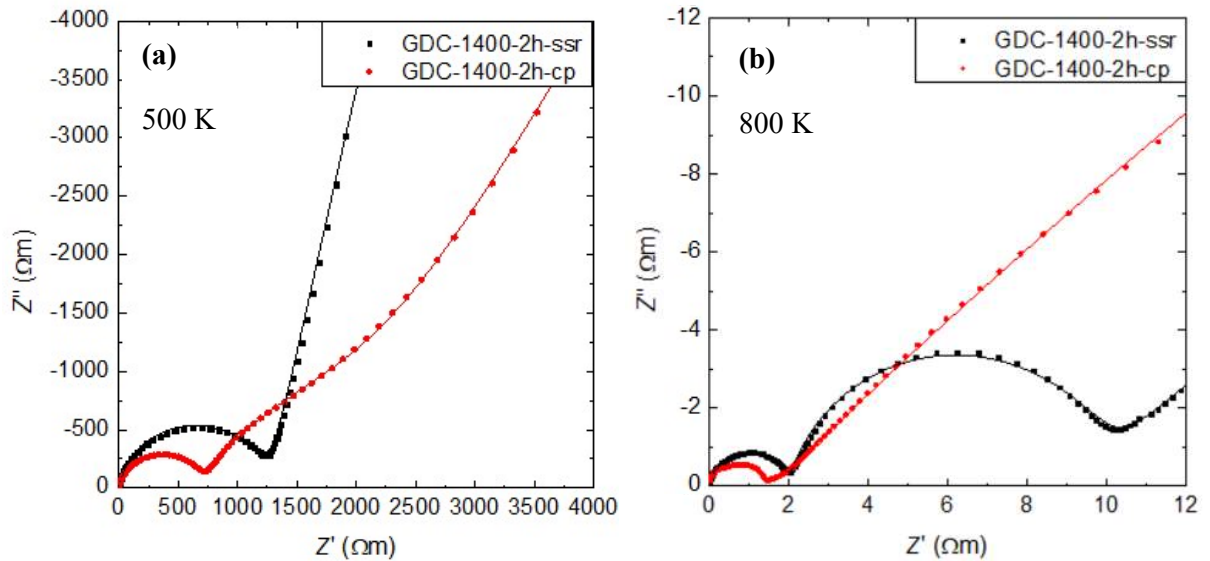


Figure 13. Nyquist plots with ZView fits of GDC-1400-2h-ssr and GDC-1400-2h-cp at temperatures of 500 K (a) and 800 K (b).

From Figure 13 (b) it is difficult to tell if what we seeing is indeed grain boundary conductivity for the second semicircle for GDC-1400-2h-cp since the semicircle is so small thus measurement by the four-electrode impedance measurement technique might be needed to obtain certainty. This would work as it removes the influence of the electrode, removing the third large curve which can be seen in above graphs and allowing for clearer view, allow for the grain boundary resistivity and thus total resistivity to be found.

From the two at 1400°C sintered samples (GDC-1400-2h-cp and GDC-1400-2h-ssr) (Figure 11) we can see the influence the powder synthesis method had on electrical conductivity. The ceramic sintered from the powder made by co-precipitation (GDC-1400-2h-cp) has higher electrical conductivity for both grain and total. The solid state reaction sample (GDC-1400-2h-ssr) also has a comparatively a very low grain boundary conductivity, which can be seen from how much the total electrical conductivity differs from the grain conductivity.

The ionic conductivity of doped ceria is changed by the synthesis method due to factors such as: from synthesis resulting powder morphology, final density of the sintered material, distribution of particle size and porosity appearing in the compacted powders. This leads to ceramics with the same composition, but varying conduction properties. [18]

From the other two GDC samples (GDC-1500-2h and GDC-1200-2h) (Figure 11), both provided by Fuel Cell Materials, and both of which were sintered from the same powder, we can see the influence

the sintering temperature had on the electrical conductivity. We notice higher electrical conductivity for both grain and total for GDC-1500-2h. It is noticeable that although the higher sintering temperature led to only a small increase in grain electrical conductivity (likely due to the increase in grain size [19]) it led to a substantial increase in total conductivity at the higher sintering temperature, hinting at a more significant improvement of grain boundary conductivity, due to likely lower grain boundary porosity. We obtained results opposite of what was obtained by Lenka et al. [20] where decreasing grain boundary conductivity was noted with the increase in grain size.

Overall, the Fuel Cell Material samples had higher conductivities than the ones provided by the University of Le Mans, most likely due to the powder synthesis method used (likely resulting in lower grain size and higher grain boundary porosity) which was not disclosed in the material data sheets.

Figure 14 illustrates and compares all the SDC samples, their electrical conductivity with relation to reciprocal temperature. Figure 14 show the Nyquist plots for those ceramics.

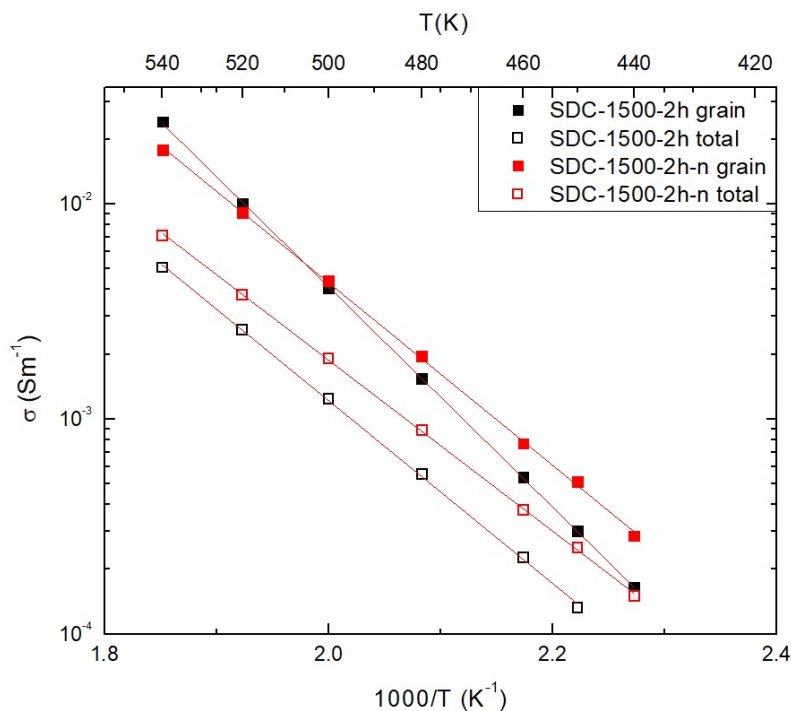


Figure 14. SDC ceramics grain and total electrical conductivity with relation to reciprocal temperature.

From the two at SDC samples (Figure 14) we can see the influence the powder BET had on electrical conductivity. While the powder having nanoscale grain size does not mean the resulting ceramic grains should be of similar size (grain sizes increase while sintering), we nevertheless see an improvement in total conductivity for the nanoscale powder.

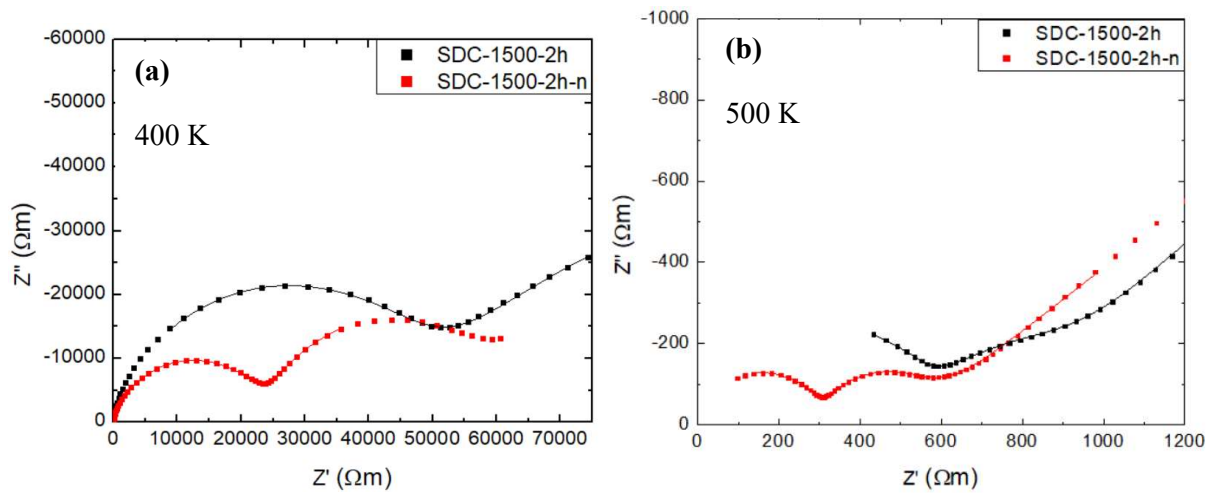


Figure 15. Nyquist plots with ZView fits of SDC-1200-2h and SDC-1200-2h-n at temperatures of 400 K (a) and 500 K (b).

From the Nyquist plots in Figure 15, we see a significant decrease in grain resistivity for the ceramic sintered from the nanoscale powder (SDC-1500-2h-n) when compared to the ceramic sintered from the larger precursor grain size powder (SDC-1500-2h).

Figure 16 illustrates and compares all the SGDC samples, their electrical conductivity with relation to reciprocal temperature. Figure 17 show the Nyquist plots for those ceramics.

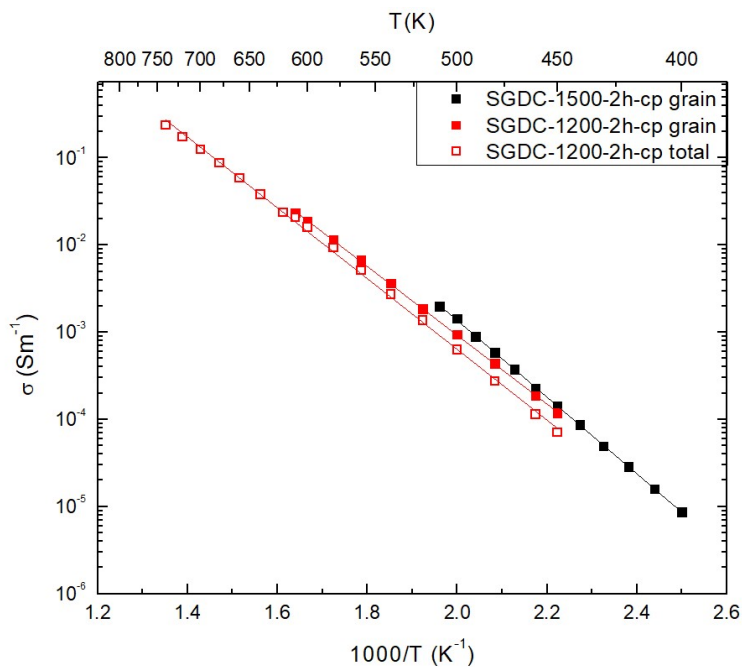


Figure 16. SGDC ceramics grain and total electrical conductivity with relation to reciprocal temperature.

It can be seen from Figure 16 and the Nyquist plots in Figure 17 that higher sintering temperature led to an increase in grain conductivity, likely due to increasing grain size. It is difficult to say any more about the sample due to the not visible total and grain resistivity from the obtained results. Additional measurements are needed to say more, perhaps usage of the four-probe impedance spectroscopy method.

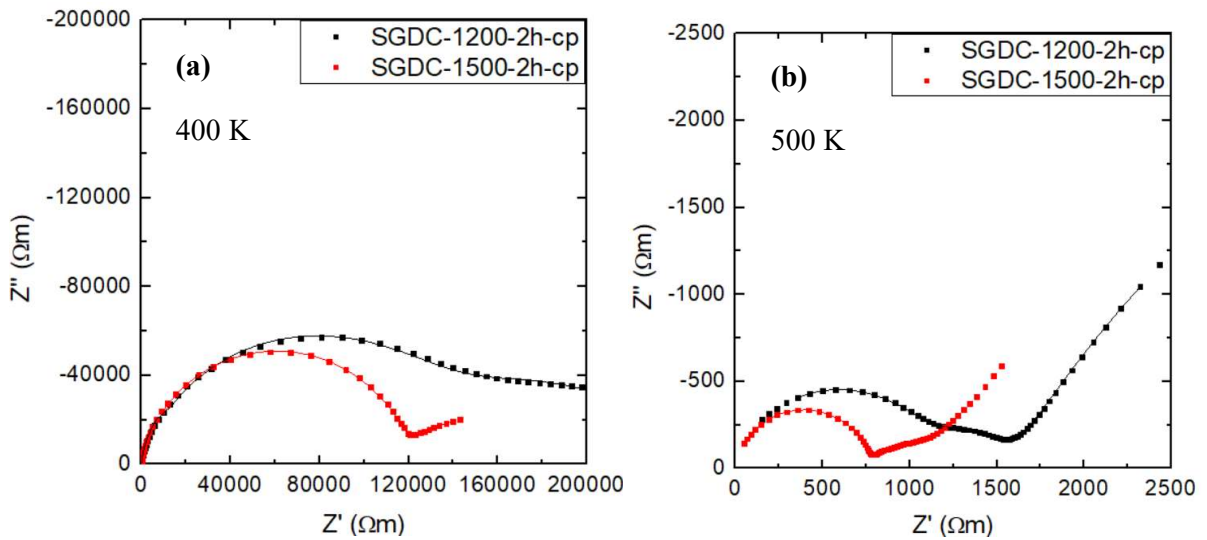


Figure 17. Nyquist plots with ZView fits of SGDC-1200-2h-cp and SGDC-1500-2h-cp at temperatures of 400 K (a) and 500 K (b).

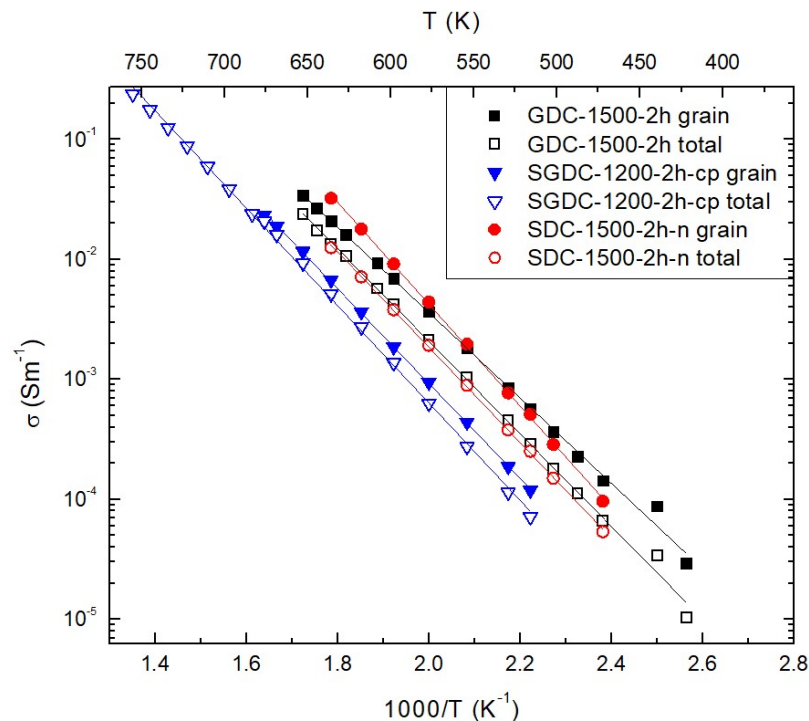


Figure 18. Highest conductivities from the investigated doped ceria ceramics. Grain and total electrical conductivity with relation to reciprocal temperature.

Figure 18 compares the highest conductivities of the three investigated types of ceramics with relation to reciprocal temperature.

As it can be seen, GDC-1500-2h showed slightly higher total conductivity than SDC-1500-2h-n, though SDC-1500-2h-n grain conductivity did rise above GDC-1500-2h at temperatures above 550°C. SGDC-1200-2h-cp showed the lowest conductivity of the three investigated ceramics.

From the literature it was expected that SGDC would have higher electrical conductivity than the other investigated doped ceria ceramics (GDC, SDC) [3,4,11,12], but this was not observed.

From these graphs of conductivity inverse temperature relation (Figures 11,14,16) and Equation 4 activation energies for grain and total electrical conductivities were obtained, as well as values of grain and total electrical conductivities at 500 K. (Table 2)

Table 2. Various ceramics - activation energies for grain ( $\Delta E_g$ ) and total ( $\Delta E_{tot}$ ) electrical conductivities and values of grain ( $\sigma_g$ ) and total ( $\sigma_{tot}$ ) electrical conductivities at 500 K.

Sample Name	$\Delta E_g$ (eV)	$\Delta E_{tot}$ (eV)	$\sigma_g$ (Sm <sup>-1</sup> )	$\sigma_{tot}$ (Sm <sup>-1</sup> )
GDC-1200-2h	0.73	0.84	2.90E-03	1.30E-03
GDC-1500-2h	0.71	0.77	3.66E-03	2.15E-03
GDC-1400-2h-ssr	0.88	1.068	8.16E-04	1.01E-05
GDC-1400-2h-cp	0.75	0.83	1.45E-03	5.25E-04
SDC-1500-2h	1.02	0.85	4.07E-03	2.27E-04
SDC-1500-2h-n	0.85	1.04	4.41E-03	1.92E-03
SGDC-1200-2h-cp	0.79	0.8	9.42E-04	6.31E-04
SGDC-1500-2h-cp	0.88	-	1.30E-03	-

Sample with the lowest total and grain activation energy similarly was the sample with the total highest electrical conductivity - GDC-1500-2h.

Similar activation energies, conductivities found in works by other researchers:

GDC10-1473-4h activation energies were found to be 0.75eV, 0.84eV for grain and total respectively [21]. Kazlauskas et al. [19] obtained the same total conductivity at 500K ( $1.3 \cdot 10^{-3}$  Sm<sup>-1</sup>) for GDC-1200-2h (the study also sintered 10% doped GDC for 2h), though noted no change in the total conductivity for GDC-1500-2h, as opposed to our noted significant increase.

It must be noted that production methods differed and that the comparison of only the final sintering time and temperature does not represent all of the factors that might influence the parameters.

## 5. Conclusions

An increase in sintering temperature from 1200°C to 1500°C in GDC and SGDC ceramics resulted in higher grain and total electrical conductivities.

SDC ceramics with higher BET had higher electrical conductivity values when sintered at the same temperature.

GDC-1400-2h-cp ceramic sintered from powder synthesised by coprecipitation had higher electrical conductivities than GDC-1400-2h-ssr ceramic sintered from powders synthesized by solid state reaction method.

Overall highest electrical conductivities and lowest electrical activation energies at 500 K were found for GDC-1500-2h with activation energies for grain and total electrical conductivities being 0.71eV and 0.77eV respectively and values of grain and total electrical conductivities of  $3.66 \cdot 10^{-3} \text{ Sm}^{-1}$  and  $2.15 \cdot 10^{-3} \text{ Sm}^{-1}$  respectively.

## 6. Bibliography

- [1] S. J. Skinner and J. A. Kilner, "Oxygen ion conductors," *Materials Today*, vol. 6, no. 3, pp. 30–37, Mar. 2003, doi: 10.1016/S1369-7021(03)00332-8.
- [2] A. V. Coles-Aldridge and R. T. Baker, "Ionic conductivity in multiply substituted ceria-based electrolytes," *Solid State Ion*, vol. 316, pp. 9–19, Mar. 2018, doi: 10.1016/j.ssi.2017.12.013.
- [3] P. C. Cajas Daza, J. L. De Almeida Ferreira, J. A. Araujo, J. A. Euzébio Paiva, R. A. Muñoz Meneses, and C. R. Moreira Da Silva, "Conductivity and microstructural evaluation of SGDC solid electrolytes synthesized by Pechini and controlled precipitation," *Boletín de la Sociedad Espanola de Cerámica y Vidrio*, vol. 61, no. 5, pp. 541–551, Sep. 2022, doi: 10.1016/J.BSECV.2021.04.003.
- [4] F. Y. Wang, B. Z. Wan, and S. Cheng, "Study on Gd<sup>3+</sup> and Sm<sup>3+</sup> co-doped ceria-based electrolytes," *Journal of Solid State Electrochemistry*, vol. 9, no. 3, pp. 168–173, Mar. 2005, doi: 10.1007/S10008-004-0575-0/FIGURES/7.
- [5] S. Omar, E. D. Wachsman, and J. C. Nino, "Higher ionic conductive ceria-based electrolytes for solid oxide fuel cells," *Appl Phys Lett*, vol. 91, no. 14, p. 144106, Oct. 2007, doi: 10.1063/1.2794725/920404.
- [6] X. Sha *et al.*, "Study on La and Y co-doped ceria-based electrolyte materials," *J Alloys Compd*, vol. 428, no. 1–2, pp. 59–64, Mar. 2009, doi: 10.1016/J.JALLCOM.2006.03.077.
- [7] N. N. Novik, V. G. Konakov, and I. Yu, "ZIRCONIA AND CERIA BASED CERAMICS AND AND MECHANICAL PROPERTIES," *Archakov Rev. Adv. Mater. Sci*, vol. 40, pp. 188–207, 2015.
- [8] X. Xu, "Ceramics in solid oxide fuel cells for energy generation," *Advances in Ceramic Matrix Composites: Second Edition*, pp. 763–788, Jan. 2018, doi: 10.1016/B978-0-08-102166-8.00031-1.
- [9] S. Anirban and A. Dutta, "Revisiting ionic conductivity of rare earth doped ceria: Dependency on different factors," *Int J Hydrogen Energy*, vol. 45, no. 46, pp. 25139–25166, Sep. 2020, doi: 10.1016/J.IJHYDENE.2020.06.119.
- [10] S. Omar and J. C. Nino, "Consistency in the chemical expansion of fluorites: A thermal revision of the doped ceria," *Acta Mater*, vol. 61, no. 14, pp. 5406–5413, Aug. 2013, doi: 10.1016/J.ACTAMAT.2013.05.029.
- [11] W. Zajac and J. Molenda, "Electrical conductivity of doubly doped ceria," *Solid State Ion*, vol. 179, no. 1–6, pp. 154–158, Mar. 2008, doi: 10.1016/J.SSI.2007.12.047.
- [12] D. R. Ou, F. Ye, and T. Mori, "Defect clustering and local ordering in rare earth co-doped ceria," *Physical Chemistry Chemical Physics*, vol. 13, no. 20, pp. 9554–9560, May 2011, doi: 10.1039/C0CP02174A.

- [13] J. A. Kilner, “Defects and conductivity in ceria-based oxides,” *Chemistry Letters*, vol. 37, no. 10, pp. 1012–1015, 2008. doi: 10.1246/cl.2008.1012.
- [14] V. F. Lvovich, *Impedance spectroscopy: applications to electrochemical and dielectric phenomena*. Wiley, 2012.
- [15] A. Kežionis *et al.*, “Four-electrode impedance spectrometer for investigation of solid ion conductors,” *Review of Scientific Instruments*, vol. 84, no. 1, Jan. 2013, doi: 10.1063/1.4774391.
- [16] A. Kežionis, S. Kazlauskas, D. Petrulionis, and A. F. Orliukas, “Broadband method for the determination of small sample’s electrical and dielectric properties at high temperatures,” *IEEE Trans Microw Theory Tech*, vol. 62, no. 10, pp. 2456–2461, 2014, doi: 10.1109/TMTT.2014.2350963.
- [17] E. Barsoukov and J. R. Macdonald, “Impedance Spectroscopy Theory, Experiment, and Applications Second Edition,” 2005.
- [18] P. C. Cajas Daza, J. L. De Almeida Ferreira, J. A. Araujo, J. A. Euzébio Paiva, R. A. Muñoz Meneses, and C. R. Moreira Da Silva, “Conductivity and microstructural evaluation of SGDC solid electrolytes synthesized by Pechini and controlled precipitation,” *Boletín de la Sociedad Española de Cerámica y Vidrio*, vol. 61, no. 5, pp. 541–551, Sep. 2022, doi: 10.1016/J.BSECV.2021.04.003.
- [19] S. Kazlauskas, A. Kežionis, T. Šalkus, and A. F. Orliukas, “Effect of sintering temperature on electrical properties of gadolinium-doped ceria ceramics,” *J Mater Sci*, vol. 50, no. 8, pp. 3246–3251, Apr. 2015, doi: 10.1007/S10853-015-8892-5.
- [20] R. K. Lenka, T. Mahata, A. K. Tyagi, and P. K. Sinha, “Influence of grain size on the bulk and grain boundary ion conduction behavior in gadolinia-doped ceria,” *Solid State Ion*, vol. 181, no. 5–7, pp. 262–267, Mar. 2010, doi: 10.1016/J.SSI.2009.12.018.
- [21] K. C. Anjaneya, G. P. Nayaka, J. Manjanna, G. Govindaraj, and K. N. Ganesha, “Preparation and characterization of  $Ce_{1-x}Gd_xO_{2\delta}$  ( $x = 0.1-0.3$ ) as solid electrolyte for intermediate temperature SOFC,” *J Alloys Compd*, vol. 578, pp. 53–59, 2013, doi: 10.1016/J.JALLCOM.2013.05.010.
- [22] D. A. Andersson, S. I. Simak, N. V. Skorodumova, I. A. Abrikosov, and B. Johansson, “Optimization of ionic conductivity in doped ceria,” *Proc Natl Acad Sci U S A*, vol. 103, no. 10, pp. 3518–3521, Mar. 2006, doi: 10.1073/PNAS.0509537103.

## Summary

Electrical properties investigation of some oxide ceramics

Gustas Levickis

Over the years a lot of efforts have been put into developing a lower operating temperature alternative to YSZ for use in SOFCs, as the high operating temperature creates a range of issues such as electrode sintering, catalyst poisoning, interfacial diffusion between electrolyte and electrode materials, thermal instability, the brittle nature of utilized materials, and the mechanical or thermal stresses arising from differing coefficients of thermal expansion. SOFCs require an electrolyte which is electron-impermeable and has a high oxygen ion conductivity.

For this application the ceramics require a high conductivity at lower operating temperatures, and thus SDC, GDC and SGDC ceramics come in as attractive options, as they are reported to have higher conductivity than the other alternatives.

The aim of this work was to investigate electrical conductivity of oxygen ion conductive ceramics and the influence of synthesis method and sintering conditions on the electrical conductivities of ceria-based ceramics.

Results were obtained by impedance spectroscopy using the ammeter-voltmeter method and the fitting of the obtained data to an equivalent circuit based on the Bauerle brick layer model. From the data obtained the following conclusions could be made:

The increase in sintering temperature from 1200°C to 1500°C in GDC and SGDC ceramics resulted in higher grain and total electrical conductivities. SDC ceramics with higher BET had higher electrical conductivity values when sintered at the same temperature. GDC-1400-2h-cp ceramic sintered from powder synthesised by coprecipitation had higher electrical conductivities than GDC-1400-2h-ssr ceramic sintered from powders synthesized by solid state reaction method. Overall highest electrical conductivities and lowest electrical activation energies at 500 K were found for GDC-1500-2h with activation energies for grain and total electrical conductivities being 0.71 eV and 0.77 eV respectively and values of grain and total electrical conductivities of  $3.66 \cdot 10^{-3} \text{ Sm}^{-1}$  and  $2.15 \cdot 10^{-3} \text{ Sm}^{-1}$  respectively.

## Santrauka

Oksidinių keramikų elektrinių savybių tyrimai

Gustas Levickis

Pastaraisiais metais nemažai pastangų buvo įdėta kuriant žemesnės darbinės temperatūros alternatyvą YSZ, skirtą naudoti SOFC. Tai yra daroma, nes esant aukštai darbinei temperatūrai SOFC kyla įvairių problemų tokių kaip elektrodų sukepinimo, katalizatoriaus užteršimo, tarpfazinės difuzijos tarp elektrolito ir elektrodų medžiagų, šiluminio nestabilumo, panaudotų medžiagų trapumo ir mechaninių ar šiluminių įtempių, atsirandančių dėl skirtingų šiluminio plėtimosi koeficientų. SOFC reikia elektrolito, kuris būtų nelaidus elektronams ir pasižymėtų dideliu deguonies vakansijų joniniu laidumu.

Šiai paskirčiai reikalingas didelis elektrinis laidumas žemesnėse temperatūrose, todėl GDC, SDC ir SGDC keramikos yra patrauklios medžiagos, nes, kaip pranešama, jų laidumas yra didesnis nei alternatyvų žemesnėse temperatūrose.

Šio darbo tikslas - ištirti deguonies jonams laidžios keramikos elektrinį laidumą ir sintezės metodo bei sukepinimo sąlygų įtaką elektriniam laidumui cerio oksido pagrindo keramikose.

Rezultatai gauti atlikus impedanso spektroskopiją ampermetro-voltmetro metodu ir gautus duomenis sutinkinus pagal Bauerle mūro-plytų modeliu pagrįstą ekvivalentinę grandinę. Iš gautų duomenų buvo padarytos šios išvados:

Padidinus sukepinimo temperatūrą nuo 1200°C iki 1500°C, GDC ir SGDC keramikose padidėjo kristalitinis ir bendras elektriniai laidumai. SDC keramikos, su aukštesne BET verte, turėjo didesnį elektrinį laidumą, kai jos buvo sukeptos toje pačioje temperatūroje. GDC-1400-2h-cp keramikų, sukeptų iš miltelių, susintetintų ko-nusodinimo metodu, elektrinis laidumas buvo didesnis nei GDC-1400-2h-ssr keramikos, sukeptos iš miltelių, susintetintų kietųjų fazių reakcijos metodu. Apibendrinus rezultatus didžiausios elektrinio laidumo ir mažiausios elektrinės aktyvacijos energijos 500 K temperatūroje buvo nustatytos GDC-1500-2h. Kristalitinio ir bendrojo elektrinio laidumo aktyvacijos energijos šiai medžiagai atitinkamai buvo 0,71eV ir 0,77eV, o kristalitinio ir bendrojo elektrinio laidumo vertės atitinkamai  $3,66 \cdot 10^{-3} \text{ Sm}^{-1}$  ir  $2,15 \cdot 10^{-3} \text{ Sm}^{-1}$ .